Neuroradiology (2015) 57:973–989
DOI 10.1007/s00234-015-1568-7

INVITED REVIEW

Bilateral symmetrical basal ganglia and thalamic lesions in children: an update (2015)

Giulio Zuccoli[1] · **Michael Paul Yannes**[2] · **Raffaele Nardone**[3] · **Ariel Bailey**[4] · **Amy Goldstein**[5]

Received: 26 March 2015 / Accepted: 15 July 2015 / Published online: 31 July 2015

Abstract
Introduction In children, many inherited or acquired neurological disorders may cause bilateral symmetrical signal intensity alterations in the basal ganglia and thalami.
Methods A literature review was aimed at assisting neuroradiologists, neurologists, infectious diseases specialists, and pediatricians to provide further understanding into the clinical and neuroimaging features in pediatric patients presenting with bilateral symmetrical basal ganglia and thalamic lesions on magnetic resonance imaging (MRI).
Results We discuss hypoxic-ischemic, toxic, infectious, immune-mediated, mitochondrial, metabolic, and neurodegenerative disorders affecting the basal ganglia and thalami.
Conclusion Recognition and correct evaluation of basal ganglia abnormalities, together with a proper neurological examination and laboratory findings, may enable the identification of each of these clinical entities and lead to earlier diagnosis.

Keywords Basal ganglia · Thalamus · Pediatrics · MRI

✉ Giulio Zuccoli
giulio.zuccoli@gmail.com

[1] Section of Neuroradiology, Children's Hospital of Pittsburgh of UPMC, 4401 Penn Avenue, Pittsburgh, PA 15224, USA

[2] Department of Radiology, University of Pittsburgh School of Medicine, Pittsburgh, PA, USA

[3] Department of Neurology, Christian Doppler Klinik, Paracelsus Medical University, Salzburg, Austria

[4] Department of Radiology, West Virginia University, Morgantown, WV, USA

[5] Department of Neurology, Section of Metabolic Disorders and Neurogenetics, Children's Hospital of Pittsburgh of UPMC, Pittsburgh, PA, USA

Introduction

The basal ganglia consist of a group of related subcortical nuclei, which, together, are responsible for multiple brain functions. Primarily, the function of the basal ganglia is to control and regulate volitional movement to ensure smooth performance. However, there are multiple other functions of the basal ganglia, including procedural learning, "routine" behaviors, and contributions to cognition and emotion. Anatomically, the basal ganglia are composed of several nuclei: the striatum (consisting of the caudate nucleus, putamen, and nucleus accumbens), the globus pallidus, the substantia nigra, and the subthalamic nucleus. Functionally, the basal ganglia have considerable connections to the cerebral cortex, thalamus, and brain stem; in fact, anatomists consider portions of the thalamus as components of the basal ganglia.

The basal ganglia are a site of high adenosine triphosphate (ATP) production and thus require a relatively disproportionate increased blood supply. Consequently, bilateral basal ganglia alterations are often observed in pathological processes affecting energy metabolism. A complete differential diagnosis of systemic and metabolic diseases would be exhaustive; therefore, understanding of the underlying pathology and imaging findings is critical for final diagnosis, treatment, and prognosis.

Both acute and progressive disorders can result in bilateral symmetrical basal ganglia alterations. Primary acute causes include hypoxic-ischemic injury (HII), infection, autoimmune disorders, and toxic encephalopathies. Subacute or progressive pathologies are usually neurodegenerative and/or metabolic in nature. The pediatric population (here defined as ages 22 days to 18 years [1]) presents unique diagnostic dilemmas, since many metabolic and genetic disorders often initially present during this time period. Identification of patterns of involvement of specific gray and/or white matter structures may aid in diagnosis.

Hypoxic-ischemic injury

A hypoxic-ischemic event (HIE) refers to any circumstance in which the aerobic demands of the neuronal parenchyma are not met. When this metabolic deficit persists, cellular death occurs. Situations that can result in a HIE are numerous, but the most common etiologies involving the basal ganglia include cardiac arrest, asphyxia, and drowning [2–4]. There are two mechanisms of injury through which any prolonged HIE can present. These include a direct ischemic insult to a structure which is asymmetrically susceptible to ischemia versus an area that receives a tenuous blood supply even under normal circumstances (termed a watershed area).

Regions historically considered asymmetrically susceptible to ischemia include the CA1 region of the hippocampus, the thalamus, cerebellum, and basal ganglia [5]. The regions supplied by both the anterior cerebral and middle cerebral arteries, as well as the middle cerebral and posterior cerebral arteries, are the areas most susceptible to "watershed" injury. While injury to specifically susceptible structures often results in both motor and cognitive deficits, injury to watershed areas often spares injury to motor-eloquent areas [6, 7].

The magnetic resonance imaging (MRI) features of cardiac arrest are characteristic of any prolonged HIE. These include acute T2 hyperintensity, late acute to subacute T1 hyperintensity, delayed T2 hypointensity, and restricted diffusion on diffusion-weighted imaging (DWI). Patients with basal ganglia hyperintensity on T2-weighted images 2 weeks following cardiac arrest represent a group with increased risk of poor outcome [8]. T1 hyperintensity occurs due to accumulation of microglia and fatty degeneration and typically becomes evident approximately 6 to 7 days following the period of cerebral ischemia (Figs. 1 and 2) [9]. T1 hyperintensity is a nonspecific finding and is characteristic of hemorrhage, protein-containing lesions, fatty lesions, calcified regions, lesions with mineral accumulation, and melanin-containing lesions [10]. However, the T1 hyperintensity following hypoxic-ischemic injury is typically bilateral and symmetric. Moreover, Wallerian degeneration of the corticospinal tracts is characteristic. The presence of delayed T2 hypointensity following cardiac arrest may be explained by the paramagnetic effect of free radicals, the presence of denatured proteins, hemorrhage, membrane lipids, and clusters of mineralized neurons. Notably, this finding is nonspecific; T2 hypointensity of the basal ganglia has also been associated with neurodegenerative disorders such as Parkinson's disease (PD), Huntington's disease (HD), and multiple sclerosis (MS) and even in healthy elderly persons due to the physiological age-related iron deposition in the basal ganglia [11]. Of note, historically, pathological correlation of these findings was termed "status marmoratus." Pathological findings included altered myelination of the putamen, caudate, and thalamus and were associated with neonatal asphyxia [12]. Magnetic resonance spectroscopy (MRS) may provide additional information regarding impairment of brain metabolism showing decreased *N*-acetyl-aspartate (NAA)/creatine (Cr) ratio and increased lactate following brain hypoxia [13].

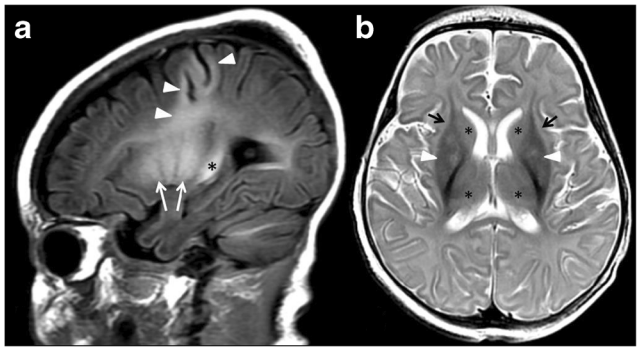

Fig. 1 Day 7 status post-cardiac arrest in a 3-month-old child. The sagittal T1-weighted image shows hyperintensity in the motor cortex and cortical-spinal tracts (**a**, *arrowheads*), putamen (**a**, *white arrows*), and optic radiations (**a**, *black asterisk*); the axial T2-weighted image shows mixed hyperintense-to-hypointense signal changes in the putamen and globus pallidus (**b**, *white arrowheads*) and hyperintensity in the caudate and thalamus, respectively (**b**, *black asterisks*) and hyperintensity in the external capsules (**b**, *black arrows*)

Neurotoxicity (iatrogenic)

Intoxication of various substances can result in bilateral basal ganglia abnormalities, such as methadone [14] and the antiepileptic drug vigabatrin [15, 16], also known as gamma-vinyl-GABA. Increasing use of methadone in withdrawal programs has increased rates of methadone poisoning in children, despite lacking epidemiological data in western countries [17].

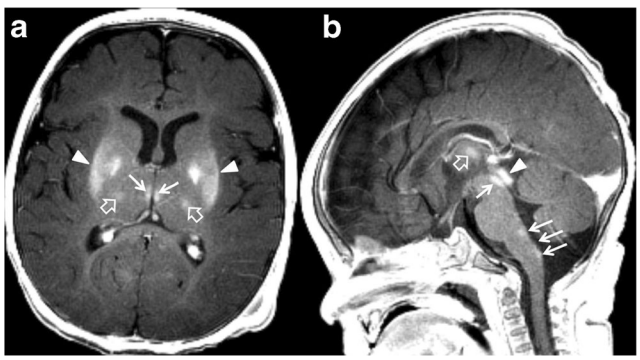

Fig. 2 A 4-month-old male 7 days status post-cardiac arrest. Post-contrast axial T1-weighted image demonstrates selective contrast enhancement of the basal ganglia with preservation of the capsules (**a**, *arrowheads*), medial thalamic nuclei (**a**, *arrows*), cortical-spinal tracts (**a**, *open arrows*). Mid-sagittal post-contrast T1-weighted image demonstrates multifocal enhancement in the central gray matter (**b**, *arrows*), thalamus (**b**, *open arrow*), and tectal plate (**b**, *arrowhead*). Areas of enhancement reflect selective blood-brain barrier damage following cardiac arrest-related brain hypoxia. Interestingly, similar anatomical brain regions are affected in Wernicke encephalopathy, secondary to thiamine (vitamin B_1) deficiency

In methadone intoxication, edema has been described in the basal ganglia, brainstem, and cerebellum, with relative preservation of the laminae medullaris of the basal ganglia [14, 17] (Fig. 3).

Transient T2 hyperintensity and restricted diffusion of the globi pallidi, thalami, dentate nuclei, and cerebral peduncles have recently been described in a significant number of young children during treatment with vigabatrin for infantile spasms. The MRI abnormalities during vigabatrin treatment seem restricted to those patients suffering from infantile spasms, and the combination of young age and high dose of vigabatrin has been proposed as a risk factor in epidemiologic studies. The MRI abnormalities may be transient [15, 16] (Fig. 4). Histopathologically, vigabatrin-related neurotoxicity demonstrates intra-myelinic edema, microvacuolation, and astrocytosis [18]. Affected regions include the bilateral globus pallidus, thalamus, dorsal brainstem, and dentate nuclei with the signal intensity alterations being usually seen on T2-weighted and or DWI/apparent diffusion coefficient (ADC) images [19]. Other agents resulting in bilateral symmetrical basal ganglia anomalies in adults may potentially be identified in the pediatric population. This includes carbon monoxide intoxication, which is characterized by restricted diffusion of the globi pallidi during the acute phase of the disease followed by pallidal vacuolation [20]. In children affected by carbon monoxide intoxication, cerebellar involvement has been recently described [21].

In children receiving total parenteral nutrition (TPN), clinical neurological manifestations have been associated with high blood concentrations of manganese [22, 23]. Manganese poisoning presents clinically with parkinsonian-like symptoms and psychological changes. Moreover, long-term parenteral administration of manganese, which bypasses the normal enteral regulatory mechanism, may cause hypermanganesemia. MRI demonstrates characteristic bilateral symmetrical increased signal intensity with T1-weighted images, without abnormalities on T2-weighted images, in the globi pallidi, anterior pituitary gland, and subthalamic nuclei [22, 24].

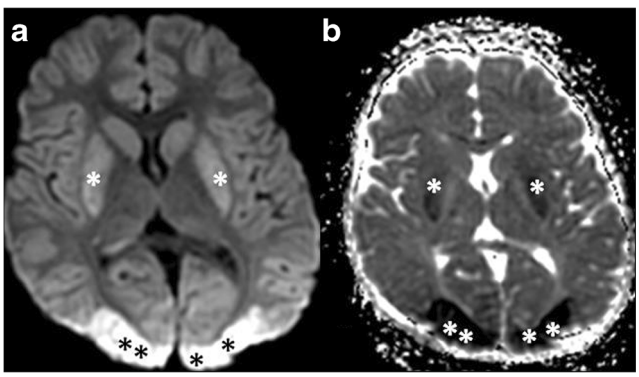

Fig. 3 Methadone intoxication in a 4-year-old patient. Cytotoxic edema is observed in the posterior putamen (*single asterisks*) and occipital (*double asterisks*) regions on DWI (**a**) and ADC map (**b**) in a 6-month-old female

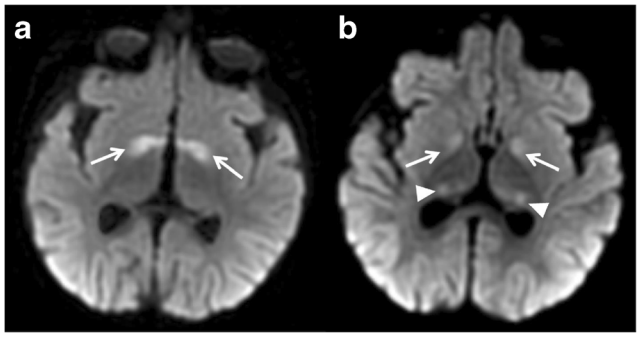

Fig. 4 Vigabatrin intoxication in a 6-month-old old patient. Bilateral pallidal (**a**, **b**, *arrows*) and thalamic (**b**, *arrowheads*) abnormalities are noted on DWI and confirmed by ADC map (not shown)

Infections

An immense diversity of pathogens can result in the clinical presentation of meningitis and/or encephalitis. However, several specific pathogens have a propensity to affect the basal ganglia. These include members of the *Herpesviridae* family of viruses, West Nile virus (WNV), Japanese encephalitis (JE), and the new-variant Creutzfeldt-Jakob disease (nvCJD), among others.

Herpesviridae refers to a large family of DNA viruses, including Epstein-Barr virus (EBV), herpes simplex virus-1 (HSV-1), herpes simplex virus-2 (HSV-2), varicella zoster virus, and cytomegalovirus. Of all the members of the *Herpesviridae* family, EBV shows the most characteristic tropism for the deep gray nuclei. T2 hyperintensity in the bilateral basal ganglia and thalami is often identified in EBV encephalitis [25–27]. Associated anomalies include the cerebral hemispheres, brainstem, and cerebellum [28]. HSV-1 is the species usually responsible for "herpes encephalitis." The radiological presentation for HSV-1 encephalitis can be incredibly variable; however, characteristically, it has a propensity to infect the unilateral or bilateral temporal lobes. Rarely, HSV-1 can lead to a vasculitis, which may result in basal ganglia involvement. Varicella Zoster Virus similarly has a relative predisposition to vasculopathy, typically involving the M1 segment of the middle cerebral artery. If the vasculopathy involves the origins of the lenticulostriate arteries, this can result in basal ganglia pathology (usually unilateral) [27]. Cytomegalovirus can affect the bilateral ganglia in the neonatal period but is fairly rare in the older population and is thus outside the scope of this discussion.

WNV infection is more commonly reported in adults than children and more commonly reported in older than younger children [29]. The lower rates of WNV disease in children, as compared to adults, may reflect, at least in part, a lack of

testing for WNV in younger symptomatic children [30, 31]. Therefore, given the potential serious neurological complications of WNV encephalitis even in children under 18 years, pediatricians must consider this infection in the differential diagnosis of children presenting with aseptic meningitis, encephalopathy, and acute flaccid paralysis. While WNV infection in adults is often asymptomatic or of limited clinical import, children seem to have a predilection for the development of encephalitis or meningitis (the so-called "West Nile neuroinvasive disease") [29]. MRI findings of WNV encephalitis demonstrate ubiquitous asymmetric alterations, including lesions in the basal ganglia and thalami. Lesions in the basal ganglia may be bilateral but are relatively rare. Restricted diffusion and patchy contrast enhancement may be observed. The spinal cord and cauda equina roots are also frequently involved [32].

The transmissible spongiform encephalopathies were, until recently, of little clinical import. However, since the description of several adolescent cases and an association with the nvCJD, interest in these rare, slowly progressive and fatal syndromes has increased among pediatricians and the general public [33]. On MRI, basal ganglia alterations in viral and spongiform encephalopathies are most often characterized by restricted diffusion either from primary viral infection or from secondary to virus-related small vessel vasculopathy and asymmetric involvement of the gray and white matter structures [26, 27, 32, 34]. Lower NAA/Cr has been described in patients affected by sporadic Creutzfeldt-Jakob disease with basal ganglia involvement showing a rapid course of the disease [35].

Influenza A (H1N1) is a major contributor to morbidity and mortality throughout the world. Although a rare complication, encephalitis secondary to influenza A has been described in association with bilateral lesions of the thalami, basal ganglia, pontine tegmentum, and periventricular white matter [22]. MRS evaluation in a cohort of 11 children affected by H1N1 encephalitis demonstrated no significant fluctuations in the major metabolites during the acute, subacute, and chronic phases of the disease with the exception for taurine and glucose. A taurine peak was noted during the subacute phase of the disease [36].

Acute necrotizing encephalopathy of childhood (ANEC) is a poorly understood entity that has been associated with a peri- and post-infectious etiology (Fig. 5). It often presents clinically initially with vague flu-like symptoms, followed by a fulminant neurologic progression. It is associated with high mortality and severe neurologic sequela. Influenza A, HSV, mycoplasma, and human herpes virus-6 (HHV-6) have all been identified as potential culprits, although some sources suggest that the causative agent is an immune reaction to the initial infectious insult. It can be characterized by multiple, symmetric lesions to the putamina, thalami, brain stem tegmentum, and white matter [37]. Interestingly, there is a lack of inflammatory cells in the affected brain parenchyma, differentiating the disease process from other entities such as acute disseminated encephalomyelitis (ADEM) (see below) [38]. Data regarding MRS findings in infectious encephalitis in children are sparse.

Autoimmunity

Many autoimmune disorders in the pediatric population can affect the basal ganglia, including post-streptococcal autoimmunity [39], *N*-methyl-D-aspartate receptor (NMDAR) antibodies [40], neuromyelitis optica (NMO)/neuromyelitis optica spectrum disorders (NMOSD) [41], and ADEM (Fig. 6) [42].

The classic post-streptococcal neurologic clinical presentation is that of Sydenham's chorea, but recently, other post-streptococcal basal ganglia-associated neurological symptoms have been described in patients who do not meet the criteria for choreiform movements, including myoclonus, dystonia, and parkinsonism [39] (Fig. 7). Although MRI imaging findings in patients with post-streptococcal findings are not consistent (and may even be normal), published abnormalities include symmetric areas of T2 hyperintensity and restricted diffusion that may involve the basal ganglia and cerebral white matter [43]. Radiologically, differentiation from acute necrotizing encephalopathy of childhood (ANEC) is impossible.

Pediatric autoimmune neuropsychiatric disorders associated with streptococcal infections

Pediatric autoimmune neuropsychiatric disorders associated with streptococcal infections (PANDAS) has been under study for many years at the National Institute of Mental Health. Although there has been controversy regarding the diagnostic criteria and temporal association with infections, there is no doubt that PANDAS is recognized as a specific disease entity involving pre-pubertal children and a dramatic, acute onset of obsessive compulsive disorder (OCD) and/or tic disorders such as Tourette syndrome. Symptoms characteristically worsen following streptococcal infections. The diagnostic criteria are as follows: (1) presence of obsessive-compulsive disorder and/or a tic disorder, (2) pediatric onset of symptoms (age 3 years to puberty), (3) episodic course of symptom severity, (4) association with group A beta-hemolytic streptococcal infection (a positive throat culture for strep or history of scarlet fever), and (5) association with neurological abnormalities (motoric hyperactivity or adventitious movements, such as choreiform movements) [44]. In addition, children may also have the following associated symptoms: (1) Attention deficit hyperactivity disorder (ADHD) symptoms (hyperactivity, inattention, fidgety), (2) separation anxiety (child is "clingy" and has difficulty separating from his/her caregivers; for example, the child may not want to be in a different room in the house from his/her parents), (3) mood changes (irritability, sadness, emotional lability), (4) sleep

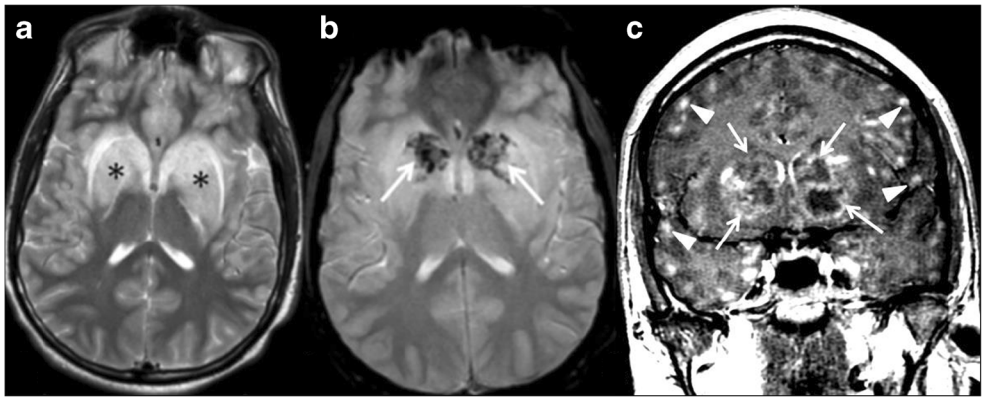

Fig. 5 Extensive basal ganglia involvement (**a**, *asterisks*) with hemorrhagic transformation (**b**, *arrows*), and necrosis is noted in a 17-year-old patient in the setting of Epstein-Barr virus (EBV) infection. Multiple cortical abnormalities associated with patchy areas of contrast enhancement (**c**, *arrowheads*) are also seen. Overall, extensive necrosis and enhancement patterns are consistent with the diagnosis of acute necrotizing encephalopathy of childhood (ANEC)

disturbance, (5) nighttime bed wetting and/or daytime urinary frequency, (6) fine/gross motor changes (e.g., changes in handwriting), and (7) joint pains [44]. MRI volumetric analysis of patients fulfilling PANDAS diagnostic criteria includes an 8 % increase in caudate volume, 7 % increase in pallidal volume, and 5 % increase in putaminal volume [45]. In addition, increase T2 and fluid-attenuated inversion recovery (FLAIR) signal can be seen in bilateral putamen and caudate nuclei [46], as well as increased microglia-mediated neuroinflammation on positron emission tomography (PET) scanning [47].

Anti-NMDAR antibody-associated encephalitis may present clinically with an acute or subacute onset of seizures, changes in consciousness, and psychiatric or neurological symptoms [40]. MRI is often unremarkable [48]. Although unusual, bilateral symmetrical basal ganglia necrosis has been described in a case of anti-NMDAR encephalitis presenting with chronic progressive dystonia [49].

Devic's syndrome, or NMO, is characterized clinically as a progressive loss of vision (optic neuritis) and spinal cord function. Antibodies against the water channel aquaporin-4 (AQP4) play a critical role. AQP4, the target antigen of NMO-IgG immunoglobulin, is a water channel protein highly concentrated in the spinal cord gray matter, periaqueductal, and periventricular regions [50]. Diagnosis is made in the presence of at least two of three criteria: MRI evidence of a contiguous spinal cord lesion three or more vertebral body segments in length, findings on brain MRI which are not consistent with multiple sclerosis (MS), and/or NMO-IgG sero-positivity [51]. Central nervous system involvement beyond the optic nerves and spinal cord is still compatible with NMO [51], although in fairness, this would be an uncommon presentation. T2 hyperintense lesions may affect the basal ganglia (and are characteristically "blurred"), hypothalamus, white matter (more frequently the frontal lobes), corpus callosum, periventricular and periaqueductal regions,

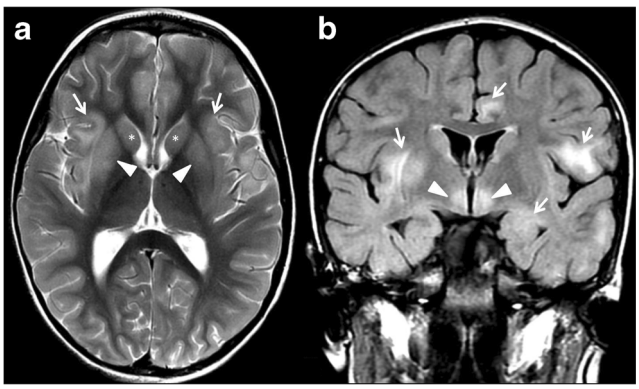

Fig. 6 A 6-year-old male suffering from acute disseminated encephalomyelitis (ADEM). Bilateral hyperintensity of the basal putamen (**a**, *arrowheads*) and caudate nucleus (**a**, *asterisks*) is noted on axial T2-weighted images. Multifocal involvement of the cortex more prominent in the frontal-insular regions is identified (**a**, **b** *arrows*). Bilateral hypothalamic hyperintensities are identified on coronal FLAIR images (**b**, *arrowheads*). MRI changes of ADEM are usually reversible

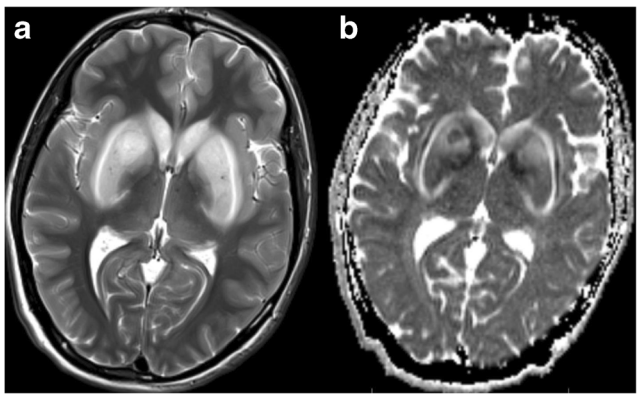

Fig. 7 A 16-year-old patient previously treated for streptococcal pharyngitis presenting unarousable. MRI obtained at admission demonstrates extensive involvement of the basal ganglia particularly at the level of the dorsal striatum on T2-weighted images (**a**) and mixed cytotoxic/vasogenic edema on ADC map (**b**). The external capsules demonstrate facilitated diffusion consistent with vasogenic edema while the claustrum demonstrates restricted diffusion consistent with cytotoxic edema

and the brainstem [41]. Interestingly, basal ganglia lesions may resolve completely over time [41].

Acute disseminated encephalomyelitis (ADEM) is a rare autoimmune disorder which also affects the brain and spinal cord. In contrast to neuromyelitis optica (NMO), ADEM is thought to be a post-infectious autoimmune response to a viral illness. Offending agents are numerous but include influenza, enterovirus, HSV, measles, and many others [52]. It has rarely been described after the administration of vaccinations in children. As stated above, it is differentiated from ANEC by the presence of inflammatory cells throughout brain parenchyma. The presentation is typically abrupt and includes fever, headache, seizures, and disparate neurological symptoms.

Imaging features suggestive of ADEM include multifocal, bilateral, asymmetric FLAIR hyperintensities in the setting of recent a viral infection or vaccination. Although white matter involvement is most common, deep gray matter nuclei can be involved in up to 50 % of cases. Occasional spinal cord involvement is possible, however, is rarely the only area of abnormality. Bilaterally symmetrical involvement would be incredibly rare. In both ADEM and NMO, vasogenic edema characterizes the acute phase of the disease, as demonstrated by ADC map [41, 42]. The presence of vasogenic edema at symptom onset may be helpful in distinguishing primary brain viral infections from autoimmunity [42].

Differentiation of ADEM from MS is often difficult in both the adult and pediatric population; however, diagnostic guidelines in children have been described [53]. In general, lesions in MS involve white matter tracts, are often periventricular, and are more frequently symmetric compared to those of ADEM. Bilateral symmetrical lesions of the basal ganglia would not be characteristic of MS in children and thus are outside the scope of this review article.

Collagen vascular diseases are systemic disorders that have their foundation in auto-immune-mediated tissue destruction. Several collagen vascular diseases can present as a neurovasculitis in the pediatric population, which can potentially affect the basal ganglia in either an asymmetric or a symmetric fashion. Patients with systemic lupus erythematosus can present with movement disorders, in which case, there are often hyperintense T1-weighted signal intensity alterations in either the unilateral or bilateral basal ganglia. Case reports have suggested a vasculitic component contributing to conditions such as dermatomyositis, Bechet's syndrome, and polyarteritis nodosa, all with variable basal ganglia involvement [54].

Inherited and acquired metabolic neurodegenerative brain disorders

Inherited metabolic brain disorders cause changes in brain metabolism and structure secondary to genetic mutations. In children, symptoms of metabolic brain disorders are often nonspecific and include seizures, hypotonia, and developmental delay. This nebulous presentation often delays diagnosis [55]. Since these disorders are progressive, the classification of neurodegenerative disorders is characterized by degree of volume loss of affected structures [55].

Lysosomal storage diseases

Lysosomal storage diseases (LSDs) are rare disorders caused by genetically transmitted lysosomal enzyme deficiencies. LSDs result when enzyme activity falls below a critical level and incompletely metabolized products accumulated within the lysosome [55]. Although the MRI findings of LSDs have not been systematically reported, there is some evidence that decreased T2 signal in the thalami may be a sign of a LSD, likely accounting for associated alteration in brain tissue viscosity [56]. Symmetric T1 hyperintensity T2 hypointensity have been described in the globi pallidi of patients affected by fucosidosis, a rare LSD caused by a decreased amount of the enzyme α-L-fucosidase [57]. More common lysosomal disorders, such as metachromatic leukodystrophy (MLD) and Krabbe disease, demonstrate abnormalities in white matter and atrophy [55].

Mitochondrial disorders

Leigh Syndrome, also known as subacute necrotizing encephalomyelopathy, is a common phenotype seen in primary mitochondrial disorders and a typically progressive neurological disease defined by specific neuropathological features often associated with brainstem and basal ganglia lesions. Leigh syndrome is an inherited disorder that usually affects infants between 3 months and 2 years of age, with rare adolescent and adult presentations. In most cases, Leigh syndrome is inherited in an autosomal recessive manner; however, there have been some reports of maternally inherited mitochondrial DNA (mtDNA) mutations. Leigh syndrome is best thought of as a phenotypic expression of multiple genetic causes, most of which involve a defect in aerobic energy production and/or oxidative stress from reactive oxygen species causing lipid peroxidation and eventual cell death. Defects range from abnormalities in the pyruvate dehydrogenase complex to the oxidative phosphorylation pathway, with a deficiency in the nuclear-encoded subunit of complex 1 of the mitochondrial respiratory chain being the most common cause of Leigh syndrome [58, 59]. However, there are at least 60 other different genetic causes of Leigh syndrome known at this time (Table 1). Restricted diffusion is classically identified in the basal ganglia in Leigh syndrome and is the most characteristic feature of the disease process [60] (Fig. 8). An abnormally low signal on T1-weighted images or hyperintensity

Table 1 Genetic causes of Leigh syndrome

Complex I: MT-ND1, 2, 3, 4, 5, 6; NDUFS1, 2, 3, 4, 7, 8; NDUFV1; NDUFA1, 2, 9, 10, 12; NDUFAF2, NDUFAF5, NDUFAF6, FOXRED1
Complex II: SDHA, SDHAF1
Complex III: UQCRQ, BCS1L, TTC19
Complex IV: SURF1, COX10, COX15, LRPPRC, NDUFA4, PET100
Complex V: MT-ATP6
PDH deficiency: PDHA1, PDHB, PDH3BP, DLD
Multiple RC defects: mtDNA deletions (Kearns-Sayre syndrome), mtDNA maintenance disorders: POLG, SUCLA, SUCLG1, mtDNA t ranslational defects: MT-TTL1, M-TTK, MT-TV, MT-TW, C12orf65, TACO1, MTFMT, GFM1, FARS2, EARS2
Defective lipid and cofactor biosynthesis: SERAC1, PDSS2, LIAS, LIPT1
Other mechanism: BTD, SLC19A3, SLC25A19, ETHE1, HIBCH

RC respiratory chain, *mtDNA* mitochondrial DNA

on T2-weighted images in the basal ganglia, periaqueductal gray matter, brainstem, and cerebellum is characteristic of this group of disorders. Involvement of the brain structures in Leigh syndrome is always bilateral and symmetric [55, 58, 59]. It has been proposed that bilateral involvement of the subthalamic nuclei and brain stem, associated with mild or even absent basal ganglia abnormalities, suggests the presence of a cyclooxygenase (COX) deficiency with underlying *SURF1* gene mutations [61]. Elevation of lactates in the basal ganglia is observed in Leigh's disease patients on MRS [62].

While most mitochondrial diseases are autosomal recessive, there are several notable exceptions. These include the pyruvate dehydrogenase complex deficiency, which is expressed in an X-linked fashion in the E1 alpha subunit of the pyruvate dehydrogenase enzyme complex. Also included are multiple mtDNA mutations, which includes Leber hereditary optic neuropathy (LHON); maternally inherited Leigh syndrome (MILS); and mitochondrial encephalomyopathy, lactic acidosis, and stroke-like episodes (MELAS).

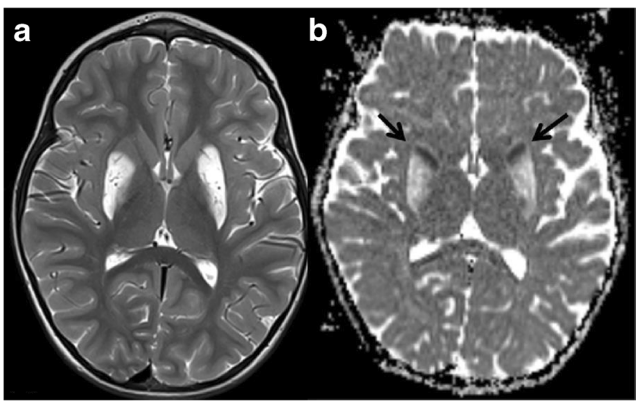

Fig. 8 A 6-year-old female patient affected by Leigh disease. Predominant vasogenic edema is noted in the bilateral putamen on T2-weighted images (**a**) and ADC map (**b**), with areas of restricted diffusion noted in the most anterior aspects of the putamen (**b**, *black arrows*)

Organic acidurias

Glutaric aciduria type 1 is an inherited disorder in which the body is unable to completely break down the amino acids lysine, hydroxylysine, and tryptophan. Excessive levels of these intermediate breakdown products, including glutaric acid, glutaryl-CoA, and glutaconic acid, can accumulate in the brain and lead to an encephalopathic crisis [63]. On T2-weighted images, hyperintensity involves both the putamina and globi pallidi in all cases. The caudate nucleus may be spared on MRI. Associated alterations include the typical "bat wing" appearance of the Sylvian fissures [64] (Fig. 9).

Methylmalonic acidemia

Methylmalonic acidemia (MMA) is an inborn error of metabolism in the organic aciduria family, which may be detected on newborn screening. Symptoms may appear at any time between the neonatal period and adulthood. Neonatal symptoms include lethargy, vomiting, hypotonia, neutropenia and thrombocytopenia, respiratory distress, ketocidosis, and hyperammonemia. Symptoms often mimic those of sepsis and delay the diagnosis. A vitamin B_{12} form of this disorder exists, so early diagnosis is important. During early childhood, symptoms may include hypotonia and developmental delay [65]. Children are at risk of having a metabolic stroke of the basal ganglia during an acute decompensation, which can result in infarction of the basal ganglia (Fig. 10) and a refractory movement disorder. Other neuroradiological findings include delayed myelination, brain stem, and cerebellar lesions [66].

Primary familial brain calcification

Primary familial brain calcification (PFBC), which had been referred to as Fahr's disease, is an autosomal dominant genetic disorder that leads to bilateral calcium deposition in the thalami, subcortical white matter, and cerebellum. Symptoms of

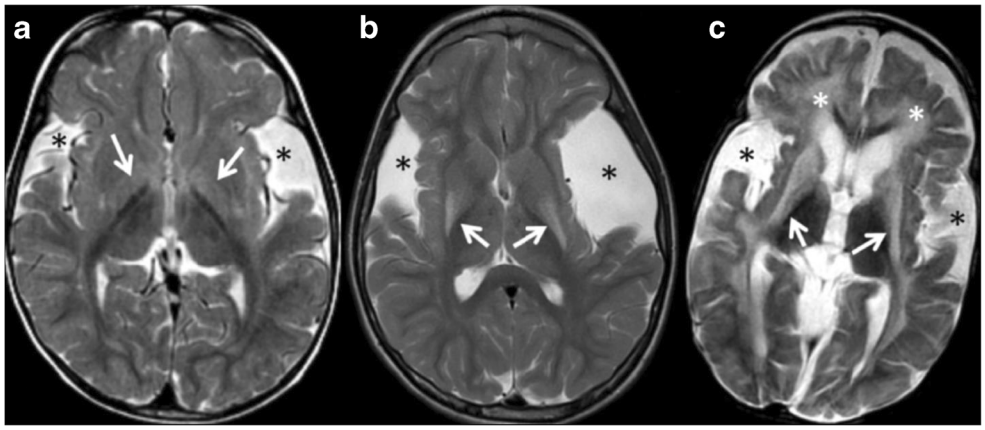

Fig. 9 Three different MRI phenotypes of glutaric aciduria type 1 (GA1). A 2-year-old patient (**a**) showing mild enlargement of the Sylvian fissures (*dark asterisks*) and mild alterations in the globus pallidus (*arrows*). A 14-month-old patient (**b**) with cystic enlargement of the Sylvian fissures (*dark asterisks*) and atrophy and gliosis in the posterior putamen (*arrows*). A 6-year-old patient (**c**) with bilateral enlargement of Sylvian fissures (*black asterisks*); extensive degeneration of the bilateral basal ganglia (*arrows*) and hemispheric white matter is noted (*white asterisks*)

dystonia, chorea, and neuropsychiatric disturbances typically present in adulthood but have been reported in children and adolescents. Fahr's disease is a progressive neurodegenerative disorder which typically presents in the fourth to fifth decade with neuropsychiatric symptoms and movement disorders, including: ataxia, dysarthria, dysphagia, migraine headaches, dementia, and epilepsy [67]. Although calcification of the basal ganglia can be seen in other disorders, such as Aicardi-Goutières syndrome, Krabbe disease, Alexander disease, mitochondrial cytopathies, and hypoparathyroidism, pattern recognition can aid the radiologist in the differential diagnosis [68].

Hypoparathyroidism

Hypoparathyroidism is the most common cause of bilateral symmetric calcification of the basal ganglia. Symptoms typically begin in childhood (earlier than in PFBC) and include tetany, weakness, seizures, paresthesias, and intellectual disability. Decreased parathyroid hormone can be idiopathic or post-surgical in etiology and results in low serum calcium and increased phosphorus. Treatment is effective, and therefore, radiographic appearance should prompt testing [69].

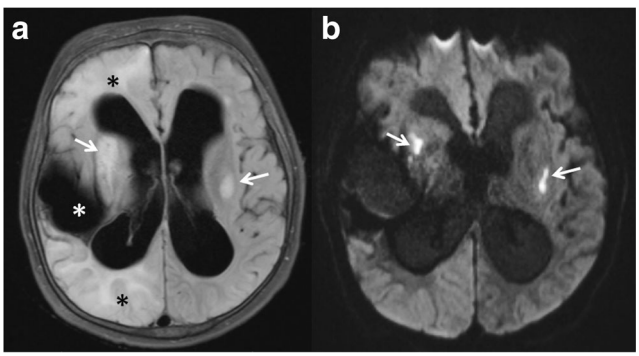

Fig. 10 A 9-year-old female affected by methyl malonic acidemia. Flair images demonstrate alterations in the bilateral putamen (**a**, *arrows*), corresponding to restricted diffusion on DWI (**b**, *arrows*). A remote stroke in the right middle cerebral artery distribution is identified (**a**, *white asterisk*). Cortical/subcortical anomalies are also seen in the right frontal lobe and right posterior periventricular white matter (**a**, *dark asterisks*)

Gangliosidoses

GM1 gangliosidosis is a lysosomal storage disorder, caused by the deficiency of the enzyme beta-galactosidase and mutations in the beta-galactosidase gene (GLB1). As a result of this enzyme deficiency, GM1 gangliosides accumulate in lysosomes, causing swelling, damage, and organ dysfunction. There are three phenotypes of the disease, distinct by age of onset and disease severity [70].

Type 1 presents in infancy and is the most common phenotype. A macular cherry red spot may be seen before the other symptoms of developmental delay and regression, hypotonia, coarsening of facial features, hepatosplenomegaly, and skeletal and cardiac involvement. Type II is a late infantile form, with corneal clouding; motor delay; and involvement of the liver, spleen, heart, and bone. Juvenile onset presents in childhood with a slower disease progression. The childhood presentations of GM1 gangliosidosis are fatal; experimental therapies are in progress. The adult form is mild and presents as dysarthria or dystonia [71]. Neuroimaging reveals progressive atrophy, abnormalities of the white matter, and nonspecific T2 hypointensity in the basal ganglia, particularly the globus pallidus. Adult-onset neuroimaging reveals hyperintensity in the putamen and/or mild cerebral atrophy [72].

GM2 gangliosidosis is a lysosomal storage disorder, caused by the deficiency of the enzyme hexosaminidase A due to mutations in HEXA. As a result of this enzyme deficiency, GM2

ganglioside, a glycosphingolipid, accumulates in lysosomes and causes a progressive neurological syndrome. The acute infantile presentation is also known as Tay-Sachs disease, which affects infants between 3 and 6 months of life with exaggerated startle response, developmental regression, seizures, blindness, spasticity, a cherry red spot on the macula, and eventual death in the first few years of life. Other forms exist with later age of onset and slower progression of symptoms. Sandhoff's disease, also known as type II GM2 gangliosidosis, is caused by a deficiency of both hexosaminidase A and hexosaminidase B. Symptoms are similar, with the addition of symptoms outside the nervous system, including hepatosplenomegaly, skeletal abnormalities, and abnormal cells in bone marrow aspirate [73]. MRI findings in Sandhoff's disease include characteristic basal ganglia and white matter T2 hyperintensity and marked T2 hypointensity in the thalami [74, 75] (Fig. 11). T2 hypointensity in the thalami is thought to reflect micro-calcifications [76]. A hexosamine peak can be identified on MRS in affected patients [77].

Aminoacidopathies

A genetic defect of the mitochondrial branched-chain alpha-ketoacid-dehydrogenase complex leads to blockage of one of the first steps in the catabolism of branched-chain amino acids (leucine, isoleucine, and valine). This disruption in normal catabolism leads to maple syrup urine disease (MSUD), which involves the accumulation of ketoacids in plasma, urine, and cerebrospinal fluid (CSF). Importantly, there is a subtype of MSUD that is responsive to thiamine (Vitamin B1) treatment [31]. The pathophysiology of MSUD is manifested through diffuse edema of myelin [78]. MRI demonstrates alterations in the basal ganglia, dorsal brainstem, cerebral peduncles, and posterior limbs of the internal capsules [79, 80] (Fig. 12). On MRS, a large methyl resonance peak at 0.9 ppm has been described in one patient affected by MMA [81, 82].

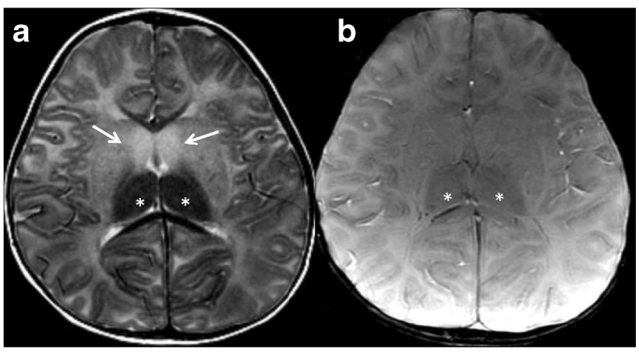

Fig. 11 A 12-month-old male affected by Sandhoff disease (GM2 gangliosidosis). There is marked T2 hyperintensity on T2-weighted images (**a**) of the caudate nucleus (*arrows*) and marked hypointensity of the thalami (*asterisks*). Diffuse white matter and putaminal hyperintensity is also noted. An unusually hypointense signal is identified in the thalami on SWI (**b**, *asterisks*)

Canavan disease, an autosomal recessive disorder arising from a deficiency of the enzyme aspartoacyclase, results in the accumulation of *N*-acetylaspartic acid in the brain. Much like MSUD, white matter involvement is characteristic. However, MRI may show an increased signal intensity in the basal ganglia and dorsal brainstem in the mild juvenile form of Canavan on T2-weighted images [83]. An NAA peak represents the hallmark MRS feature of Canavan disease [84].

Wilson disease

Wilson disease, also known as hepatolenticular degeneration, is a rare and treatable autosomal recessive disorder that involves an excessive accumulation of copper. Copper accumulates primarily in the liver and brain, resulting in mainly hepatic and neurological sequela [85–89]. The Kayser-Fleischer ring, a darkened brown ring at the junction of the cornea with the sclera, is a distinctive characteristic of Wilson disease. However, Kayser-Fleischer rings are observed less often in the pediatric age group, because they result from the chronic deposition of copper [32, 34]. The neurological form of Wilson disease clinically presents with the classic "wing-beating tremor," dysarthria, ataxia, and rigidity. Psychiatric symptoms are variably observed in adults [90, 91]; however, this presentation is less common in children and is reported at rates of 4 to 12 % [86, 92]. On MRI, the basal ganglia, specifically the putamina, caudate nuclei, and globi pallidi, are hyperintense on T1-weighted (Fig. 13) and T2-weighted images. The white matter may show progressive T2 hyperintensity during the late course of Wilson Disease. Corpus callosum abnormalities have also been described [55]. In the neurological Wilson disease phenotype Choline (Cho)/Cr, Glutamine (Glx)/Cr ratio levels inversely correlate with the clinical status of the patients [93].

Huntington's disease

Huntington's disease (HD) is an autosomal-dominant progressive neurodegenerative disorder, with an incidence of 5–10 per 100,000 individuals. While the classic form of HD has an onset in adulthood, juvenile HD is a rare clinical entity characterized by disease onset before the age of 21. It accounts for <10 % of HD patients. Adult-onset HD usually presents with choreiform movements, progressive dementia, and behavioral abnormalities; however, Juvenile HD can present with myoclonus, seizures, behavioral problems, and parkinsonian features. Importantly, choreiform movements are often absent. Transmission of juvenile HD is paternal in 80–90 % of cases. In JHD, distinguishing neuroimaging findings are represented by caudate and cerebellar atrophy [94]. Diffusely elevated glutamate and low Cr levels in the basal ganglia have been described in Juvenile HD [95].

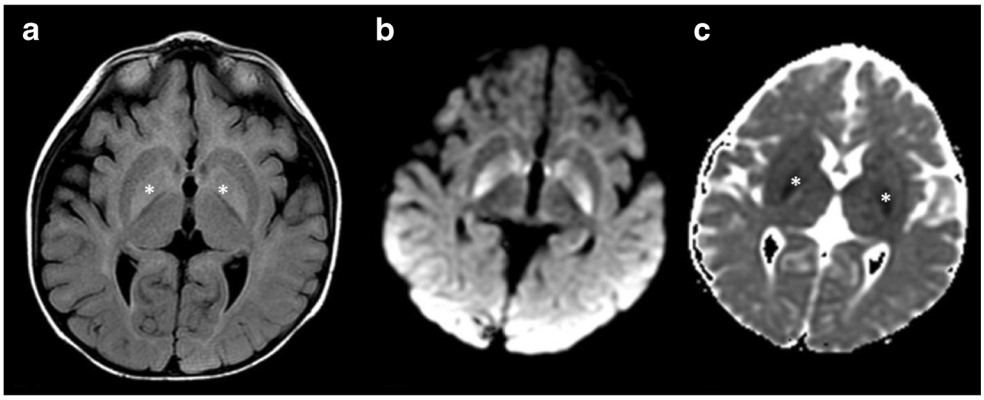

Fig. 12 A 2-year-old male affected by maple syrup disease (MSUD). FLAIR images (**a**) show alterations in the globus pallidus without volume loss (*asterisks*). DWI (**b**) and ADC map (**c**, *asterisks*) images show cytotoxic edema in the globus pallidus

Infantile bilateral striatal necrosis

Infantile bilateral striatal necrosis is a rare autosomal recessive disorder, which, like Leigh syndrome, represents a common phenotypic expression of multiple genetic derangements. Clinical features are nonspecific, including choreoathetosis, dystonia, spasticity, and mental regression. Pathological findings include severe gliosis and neuronal loss. Imaging correlates include bilateral symmetrical volume loss and T2 hyperintensity of the caudate nuclei, putamina, and, rarely, the globi pallidi. Usually, patients who are diagnosed early will have putamina involvement versus those that are diagnosed later will have caudate involvement [11]. A late diagnosis can make it difficult to distinguish from Juvenile HD. Additionally, features can be markedly similar to acute necrotizing encephalopathy of childhood (ANEC); however, a robust recent past medical history will often clinch the diagnosis [96]. Small studies have suggested a partial treatment response to biotin [97]; because of this, some sources have suggested that this disease is actually the same as the biotin-responsive basal ganglia disease spectrum (see below) [98].

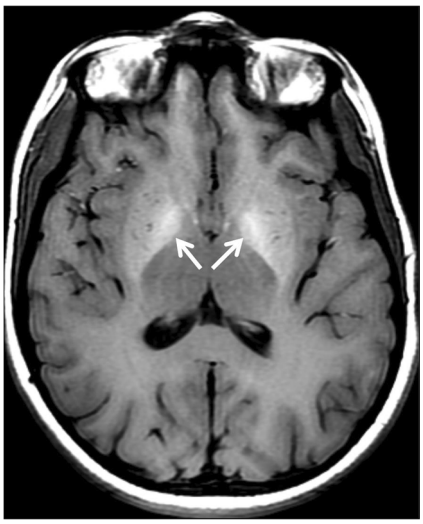

Fig. 13 A 13-year-old patient with Wilson disease showing spontaneous T1 hyperintensity in the basal ganglia, more pronounced in the bilateral globus pallidus (*arrows*)

Neurodegeneration with brain iron accumulation spectrum disorders

The so-called neurodegeneration with brain iron accumulation (NBIA) spectrum disorders encompass a phenotypic expression of approximately ten genetic mutations. The combination of spasticity, dystonia, neuropsychiatric symptoms, and cerebellar atrophy should raise suspicion for these disorders. The disease is typically progressive and can present from infancy to adulthood. The value of standard MRI sequences in the diagnosis of NBIA spectrum has gained importance over time, particularly after the introduction of susceptibility-weighted imaging (SWI) [99]. Abnormalities in the basal ganglia may not be apparent on standard imaging sequences such as T2- and T1-weighted sequences, but excessive iron accumulation may be noted on SWI, and the exact location of iron accumulation correlates with the genotype.

The most commonly diagnosed NBIA disorder is pantothenate kinase-associated neurodegeneration (PKAN) and is caused by a mutation in the gene encoding pantothenate kinase 2 (PANK2). In addition to the clinical characteristics of any NBIA, pigmentary retinopathy is often present in children [100]. The iron deposition and destruction of the globus pallidus in this disease give rise to a characteristic and virtually pathognomonic MRI abnormality, called the "eye-of-the-tiger" sign: T2-weighted hypointense signal in the globus pallidus with a central region of hyperintensity (Fig. 14). The MRI signal intensity abnormalities in the globus pallidus can distinguish patients with mutations in PANK2 from those lacking a mutation, even in the early stages of disease [101].

In PLA2G6-associated neurodegeneration (PLAN), also known as infantile neuroaxonal dystrophy (INAD), typical neuroimaging features include cerebellar atrophy and optic nerve atrophy. Brain iron accumulation in the globus pallidus

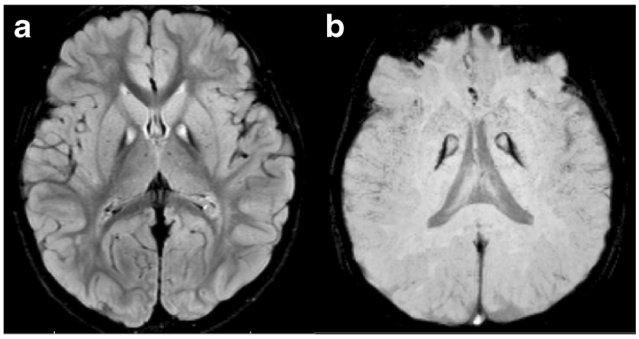

Fig. 14 A 4-year-old patient with pantothenate kinase-associated neurodegeneration (PKAN) showing the typical eye-of-the-tiger appearance of the globus pallidus on FLAIR (**a**) and SWI (**b**)

and substantia nigra is variable and seen in about half of these cases [102, 103] (Fig. 15). Neuroimaging of PLAN/INAD shows marked cerebellar atrophy in addition to iron accumulation of the globus pallidus and substantia nigra [104]. Finally, although most of the NBIA disorders are inherited in an autosomal recessive manner, the only X-linked NBIA disorder is the disease entity known as beta-propeller protein-associated neurodegeneration (BPAN) [105].

Wernicke encephalopathy

Although commonly considered as a condition peculiar to malnourished adults who suffer from alcohol abuse, a variety of genetic mutations affecting thiamine metabolism can result in the phenotypic expression of Wernicke encephalopathy [106]. Changes in consciousness are nonspecific in acutely ill patients. For this reason, reliance on the "classic triad" of ataxia, global confusion, and opthalmoplegia has been shown to be misleading.

The body's reserve of thiamine, which is approximately 30–50 mg, can be depleted in 2–3 weeks [106]. Carbohydrate intake, infection, and physical activity all increase thiamine metabolism. In brain regions with high metabolic requirements and high thiamine turnover, a lack of thiamine may cause tissue injury through inhibition of proper metabolism. A search for any cause of malnutrition or unbalanced nutrition in the clinical history is of utmost importance. Abnormal biochemical processes are potentially reversible, so treatment should be started as soon as possible. At autopsy, the incidence of Wernicke encephalopathy in the general population is about 0.8–2.8 %. However, post-mortem studies indicate that Wernicke encephalopathy is underdiagnosed in the pediatric population. In children, over 58 % of pathologically proven cases have been missed at routine clinical examination. Of note, young patients being treated for acute leukemia are at an increased risk for developing Wernicke encephalopathy [107–110].

Frontal cortex, basal ganglia, and diffuse brainstem involvement in Wernicke encephalopathy all indicate a poor prognosis, even when thiamine is administered promptly. In infants suffering from Wernicke encephalopathy, there is preferential damage to the frontal lobes, followed by the basal ganglia [97]. Since MRI is utilized in most cases of suspected pediatric Wernicke encephalopathy, it is important to be aware of characteristic and localized findings in the thalami, mammillary bodies, periaqueductal gray matter, basal ganglia, and the cranial nerve nuclei [111].

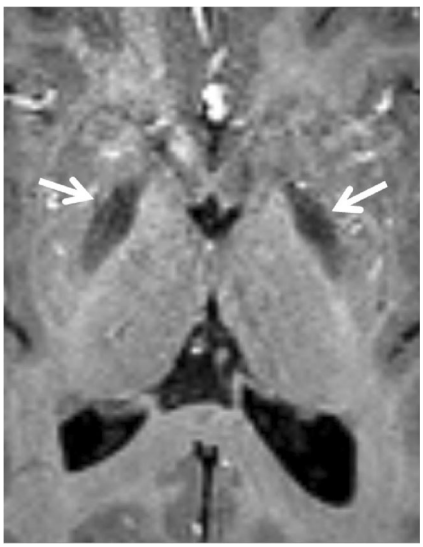

Fig. 15 A 3-year-old patient affected by PLA2G6-associated neurodegeneration (PLAN) showing excessive iron accumulation in the globus pallidus on SWI (*arrows*)

Biotin-responsive basal ganglia disease

Biotin-responsive basal ganglia disease is a rare autosomal recessive disorder, caused by mutations in the *SLC19A3* gene, which encodes a thiamine transporter [98, 112]. Biotin-responsive basal

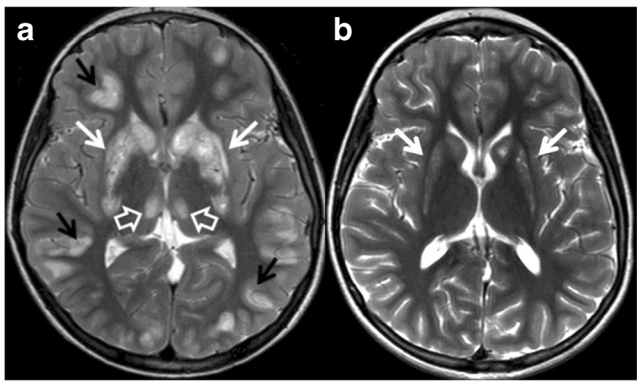

Fig. 16 Biotin-responsive basal ganglia disease (BBGD) in a 4-year-old patient. Cortical (**a**, *black arrows*), basal ganglia (**a**, *white arrows*), and thalami (**a**, *open arrows*) alterations are seen in the acute phase of the disease resulting in basal ganglia atrophy (**b**, *arrows*) at follow-up. Courtesy of Prof. Brahim Tabarki (with permission)

Table 2 Bilateral symmetrical lesions in the basal ganglia and thalami: primary involvement and common anatomical associations in affected children

	Primary involvement	Anatomical associations/signal features
Hypoxia		
	BG and Th	Brain cortex, cerebellum, hippocampus white matter, brainstem, subthalamic nuclei; variable RD, ↑T2, ↑T1
Neurotoxicity		
Vigabatrin	GP and Th	Dorsal brainstem and dentate nuclei; RD, ↑T2
Carbon monoxide	GP (internus)	Supratentorial white matter and cerebellum; RD (acute phase), vacuolation ↑T2 (chronic phase)
Manganese	BG	Subthalamic nuclei, anterior pituitary gland; ↑T1
Methadone	BG	Brainstem and cerebellum; RD
Vigabatrin	GP and Th	Brainstem and dentate nuclei; RD
Infectious/post-infectious		
Epstein-Barr virus	BG and Th	Cerebral hemispheres, brainstem and cerebellum; RD, enhancement
West Nile virus	BG and Th	Asymmetric lesions in cerebral lobes, brainstem and cerebellum; meningeal enhancement and RD
Creutzfeldt-Jakob disease (CJD)	BG and Th (*pulvinar sign*)	Brain cortex (*ribbon sign*) and brainstem; RD
Influenza A encephalitis	BG and Th	Pontine tegmentum and periventricular white matter; RD and enhancement
Acute necrotizing encephalopahty (ANEC)	Th and putamen	Multifocal asymmetric necrotizing brain lesions; RD and contrast enhancement (ring-like), hemorrhage
Post-streptococcal disease	BG	Cerebral white matter; RD
Autoimmune		
Anti-NMDA receptor encephalitis	BG	Hippocampus; MRI may also be negative
Neuromyelitis optica	BG (rare)	Hypothalamus, white matter (more frequently in frontal lobes), corpus callosum, periventricular and periaqueductal regions, and brainstem; VE
Acute disseminated encephalomyelitis (ADEM)	BG	Multifocal cortical subcortical, brainstem and cerebellum; VE
Inborn errors of metabolism		
Lysosomal storage disorders	GP and Th	BG+Th T2↓ and T1↑; subcortical white matter T2↑ in Fucosidosis. Th ↓T2; white matter ↑T2 in Sandhoff disease
Mitochondrial disorders	BG and Th	Leigh syndrome: periaqueductal gray matter, brainstem, and cerebellum; ↓T1,↑T2, RD
Organic acidurias (glutaric aciduria type 1)	Putamen and GP	Wide Sylvian fissures; caudate typically spared; RD, ↑T2
Methyl malonic aciduria (MMA)	BG	Abnormal myelination, brain stem and cerebellar lesions; ↑T2
Primary familial brain calcification (PFBC)	Th	Calcifications in subcortical white matter and cerebellum; ↓SWI
Amino acidopathy (MSUD)	BG	Diffuse edema of myelin, dorsal brainstem, cerebral peduncles, and posterior limbs of the internal capsules; RD, ↑T2
Canavan disease (CD)	BG	White matter and dorsal brainstem; ↑T2, increased NAA
Wilson disease (WD)	BG	Corpus callosum (splenium); ↑T1
Juvenile Huntington disease (JHD)	BG	Cerebellar atrophy
Neurodegeneration with brain iron accumulation spectrum disorders (NBIAs)	BG and SN	"*Eye of the tiger*" in PKAN Iron accumulation and cerebellar atrophy indicates PLAN or BPAN ↓SWI
Wernicke encephalopathy (WE)	BG and Th (medial nuclei and periventricular regions of third ventricle)	Mammillary bodies, periaqueductal gray matter, cranial nerve nuclei; RD, ↑T2, contrast enhancement
Biotin-responsive basal ganglia disease (BBGD)	BG and Th (medial nuclei)	Scattered cortical lesions (cerebral hemispheres and cerebellum), brainstem; VE

Table 2 (continued)

	Primary involvement	Anatomical associations/signal features
Urea cycle disorders/hyperammonemia		Insular cortex; cingulate gyrus; RD, ↑T2
Infantile bilateral striatal necrosis (IBSN)	BG (striatum)	Putamen (early phase); caudate (late phase); GP rarely involved; RD, ↑T2
Succinic semialdehyde dehydrogenase (SSADH) deficiency	GP	White matter hypomyelination; dentate nucleus; ↑T2

BG basal ganglia, *Th* thalamus, *GP* globus pallidus, *RD* restricted diffusion, *VE* vasogenic edema, *SWI* susceptibility weighted images, *T1* T1-weighted images, *T2* T2-weighted images, Bright signal↑; Dark signal↓, *NAA N*-acetyl-aspartate, *SN* substantia nigra, *PKAN* pantothenate kinase-associated neurodegeneration, *PLAN* PLA2G6-associated neurodegeneration, *BPAN* beta-propeller protein-associated neurodegeneration

ganglia disease frequently manifests in childhood, resulting in subacute episodes of encephalopathy, leading to coma, seizures, and extrapyramidal manifestations [113]. In those who are not timely treated, death and neurologic deficits such as dystonia, mental retardation, and epilepsy have been described. MRI typically demonstrates symmetric and bilateral hyperintense lesions on T2-weighted sequences in the caudate nucleus and putamina, medial nuclei of the thalami, infra-and supratentorial brain cortices, and dorsal brainstem (Fig. 16). The acute crises may be characterized by vasogenic edema as seen on the ADC map [113]. In patients with chronic disease, atrophy and gliosis are observed in the affected region. Early treatment with a combination of biotin and thiamine is lifesaving in patients with biotin-responsive basal ganglia disease, resulting in clinical and neuroradiologic improvement. Thus, biotin-responsive basal ganglia disease is an important consideration and treatable condition in the differential diagnosis of mitochondrial disorders. Biotin-responsive basal ganglia disease can also often be mistaken for Wernicke encephalopathy, secondary to the fact that both can present with bilateral medial thalamic nuclei involvement in the typical "butterfly" morphology [110, 111, 113]. However, biotin-responsive basal ganglia disease often more extensively involves the cerebellar and hemispheric cortices than Wernicke encephalopathy, and basal ganglia atrophy is usually more pronounced in biotin-responsive basal ganglia disease than Wernicke encephalopathy [113]. Furthermore, the mammillary bodies and brainstem nuclei are almost always involved in Wernicke encephalopathy versus less consistent involvement in biotin-responsive basal ganglia disease [111, 114].

Urea cycle defects

The urea cycle disorders are a family of several disorders, resulting from deficiencies of the enzymes important for the urea cycle, which metabolizes waste nitrogen from protein. Neonatal presentations include vomiting, seizures, and coma from hyperammonemia and resulting cerebral edema. Hyperammonemia in the newborn can mimic sepsis or hypoxic-ischemic encephalopathy, and neuroimaging may be similar to that seen in HIE, with lacunar infarcts and abnormalities of white matter in addition to basal ganglia injury [115]. Neuroradiology plays an important role in helping to determine prognosis and ultimate neurocognitive outcomes, although MRI may lag behind the clinical symptoms. On DWI/ADC, restricted diffusion often involves the cortex diffusely and can be reversible with therapy [116]. Additional imaging, including MRS diffusion tensor imaging (DTI), and functional magnetic resonance imaging (fMRI) are being utilized in urea cycle defects [116–118]. Increased glutamine and decreased myoinositol may be observed [119].

Others

Central pontine and extrapontine myelinolysis (CPM-EPM) represents a demyelination syndrome presenting with spastic tetraparesis, quadriparesis, pseudobulbar paralysis, coma, seizures, and the "locked in" syndrome. CPM-EPM is usually associated with aggressive and rapid correction of hyponatremia. However, it has also been described in association with Wilson Disease, diabetes mellitus, autoimmune disorders including systemic lupus erythematosus, post-liver transplantion, infections, lymphoma, leukemia, and electrolyte imbalances [120]. Neuroimaging findings include increased T2 signal in the pons and basal ganglia with restricted diffusion [121].

Pediatric neurotransmitter disorders encompass a heterogeneous group of inherited neurometabolic diseases [122]. In succinic semialdehyde dehydrogenase (SSADH) deficiency, brain MRI may reveal hypomyelination or hyperintensities on T2-weighted images in multiple brain regions, but most commonly in the globus pallidus [123–125].

The main neuroanatomical associations and imaging findings in children presenting with signal intensity alterations in the basal ganglia and/or thalami are resumed in Table 2.

Conclusion

We have reviewed many causes of bilateral symmetrical basal ganglia imaging abnormalities that present with neurological symptoms. Both the neurologist and neuroradiologist need to be aware of the constellation of findings associated with these

disorders to allow proper diagnosis. Clinical symptoms and laboratory tests usually guide the differential diagnosis; however, neuroimaging findings may provide clues in diagnosis and prognosis. More specifically, bilateral symmetrical basal ganglia abnormalities associated with bilateral symmetrical brainstem and cortical alterations point to the diagnosis of disorders of brain metabolism in the appropriate clinical and laboratory setting. On the other hand, asymmetrical brainstem and cortical involvement is usually associated with infectious or para-infectious (autoimmune) etiologies.

Acknowledgments In memory of my dear friend, Massimo Gallucci, Professor of Neuroradiology.

Ethical standards and patient consent We declare that this manuscript does not contain clinical studies or patient data.

Conflict of interest We declare that we have no conflict of interest.

References

1. Williams K, Thomson D, Seto I, StaR Child Health Group et al (2012) Standard 6: age groups for pediatric trials. Pediatrics 129(Suppl 3):S153–S160. doi:10.1542/peds.2012-0055I
2. Tian N, Shaw EC, Zack M et al (2015) Cause-specific mortality among children and young adults with epilepsy: results from the U.S. National Child Death Review Case Reporting System. Epilepsy Behav 45:31–34. doi:10.1016/j.yebeh.2015.02.006
3. Wallis BA, Watt K, Franklin RC et al (2015) Drowning mortality and morbidity rates in children and adolescents 0-19yrs: a population-based study in Queensland, Australia. PLoS One 10, e0117948. doi:10.1371/journal.pone.0117948
4. Bhalala US, Koehler RC, Kannan S (2014) Neuroinflammation and neuroimmune dysregulation after acute hypoxic-ischemic injury of developing brain. Front Pediatr 2:144. doi:10.3389/fped.2014.00144
5. Dirnagl U, Iadecola C, Moskowitz MA (1999) Pathobiology of ischaemic stroke: an integrated view. Trends Neurosci 22:391–397
6. Ginsberg MD, Hedley-Whyte E, Richardson EP Jr (1976) Hypoxic-ischemic leukoencephalopathy in man. Arch Neurol 33:5–14. doi:10.1001/archneur.1976.00500010007002
7. Panigrahy A, Blüm S (2007) Advances in magnetic resonance neuroimaging techniques in the evaluation of neonatal encephalopathy. Top Magn Reson Imaging 18:3–29. doi:10.1097/RMR.0b013e318093e6c7
8. Fink EL, Panigrahy A, Clark RSB et al (2013) Regional brain injury on conventional and diffusion weighted MRI is associated with outcome after pediatric cardiac arrest. Neurocrit Care 19:31–40. doi:10.1007/s12028-012-9706-0
9. Aoe H, Takeda Y, Kawahara H et al (2006) Clinical significance of T1-weighted MR images following transient cerebral ischemia. J Neurol Sci 241:19–24. doi:10.1016/j.jns.2005.10.013
10. Cakirer S, Karaarslan E, Arslan A (2003) Spontaneously T1-hyperintense lesions of the brain on MRI: a pictorial review. Curr Probl Diagn Radiol 32:194–217. doi:10.1016/S0363-0188(03)00026-4
11. Bekiesinska-Figatowska M, Mierzewska H, Jurkiewicz E (2013) Basal ganglia lesions in children and adults. Eur J Radiol 82:837–849. doi:10.1016/j.ejrad.2012.12.006
12. Malamud N (1950) Status marmoratus; a form of cerebral palsy following either birth injury or inflammation of the central nervous system. J Pediatr 37:610–619
13. Nucci-da-Silva MP, Amaro E (2009) A systematic review of Magnetic Resonance Imaging and Spectroscopy in brain injury after drowning. Brain Inj 23:707–714. doi:10.1080/02699050903123351
14. Zanin A, Masiero S, Severino MS et al (2010) A delayed methadone encephalopathy: clinical and neuroradiological findings. J Child Neurol 25:748–751. doi:10.1177/0883073809343318
15. Wheless JW, Carmant L, Bebin M et al (2009) Magnetic resonance imaging abnormalities associated with vigabatrin in patients with epilepsy. Epilepsia 50:195–205. doi:10.1111/j.1528-1167.2008.01896.x
16. Pearl PL, Vezina LG, Saneto RP et al (2009) Cerebral MRI abnormalities associated with vigabatrin therapy. Epilepsia 50:184–194. doi:10.1111/j.1528-1167.2008.01728.x
17. Bazmamoun H, Fayyazi A, Khajeh A et al (2014) A study of methadone-poisoned children referred to Hamadan's Besat Hospital/Iran. Iran J Child Neurol 8:34–37
18. Preece NE, Houseman J, King MD et al (2004) Development of vigabatrin-induced lesions in the rat brain studied by magnetic resonance imaging, histology, and immunocytochemistry. Synapse 53:36–43. doi:10.1002/syn.20038
19. Dracopoulos A, Widjaja E, Raybaud C et al (2010) Vigabatrin-associated reversible MRI signal changes in patients with infantile spasms. Epilepsia 51:1297–1304. doi:10.1111/j.1528-1167.2010.02564.x
20. Beppu T (2014) The role of MR imaging in assessment of brain damage from carbon monoxide poisoning: a review of the literature. Am J Neuroradiol 35:625–631. doi:10.3174/ajnr.A3489
21. Velioglu M, Gümüş T, Hüsmen G (2013) Cerebellar lesions in the acute setting of carbon monoxide poisoning. Emerg Radiol 20:255–257. doi:10.1007/s10140-013-1108-x
22. Ono J, Harada K, Kodaka R et al (1995) Manganese deposition in the brain during long-term total parenteral nutrition. JPEN J Parenter Enteral Nutr 19:310–312
23. Fell JM, Reynolds AP, Meadows N et al (1996) Manganese toxicity in children receiving long-term parenteral nutrition. Lancet 347:1218–1221
24. Quaghebeur G, Taylor WJ, Kingsley DP et al (1996) MRI in children receiving total parenteral nutrition. Neuroradiology 38:680–683
25. Häusler M, Ramaekers VT, Doenges M et al (2002) Neurological complications of acute and persistent Epstein-Barr virus infection in paediatric patients. J Med Virol 68:253–263. doi:10.1002/jmv.10201
26. Phowthongkum P, Phantumchinda K, Jutivorakool K, Suankratay C (2007) Basal ganglia and brainstem encephalitis, optic neuritis, and radiculomyelitis in Epstein-Barr virus infection. J Infect 54:e141–e144. doi:10.1016/j.jinf.2006.09.007
27. Baskin HJ, Hedlund G (2007) Neuroimaging of herpesvirus infections in children. Pediatr Radiol 37:949–963. doi:10.1007/s00247-007-0506-1
28. Abul-Kasim K, Palm L, Maly P, Sundgren PC (2009) The neuroanatomic localization of Epstein-Barr virus encephalitis may be a predictive factor for its clinical outcome: a case report and review of 100 cases in 28 reports. J Child Neurol 24:720–726
29. Lindsey NP, Hayes EB, Staples JE, Fischer M (2009) West Nile virus disease in children, United States, 1999-2007. Pediatrics 123:e1084–e1089. doi:10.1542/peds.2008-3278
30. Civen R, Villacorte F, Robles DT et al (2006) West Nile virus infection in the pediatric population. Pediatr Infect Dis J 25:75–78
31. Weber IB, Lindsey NP, Bunko-Patterson AM et al (2012) Completeness of West Nile virus testing in patients with meningitis and encephalitis during an outbreak in Arizona, USA.

Epidemiol Infect 140:1632–1636. doi:10.1017/S0950268811002494
32. Ali M, Safriel Y, Sohi J et al (2005) West Nile virus infection: MR imaging findings in the nervous system. AJNR Am J Neuroradiol 26:289–297
33. Whitley RJ, MacDonald N, Asher DM (2000) American Academy of Pediatrics. Technical report: transmissible spongiform encephalopathies: a review for pediatricians. Committee on Infectious Diseases. Pediatrics 106:1160–1165
34. Zeng H, Quinet S, Huang W et al (2013) Clinical and MRI features of neurological complications after influenza A (H1N1) infection in critically ill children. Pediatr Radiol 43:1182–1189. doi:10.1007/s00247-013-2682-5
35. Kim JH, Choi BS, Jung C et al (2011) Diffusion-weighted imaging and magnetic resonance spectroscopy of sporadic Creutzfeldt-Jakob disease: correlation with clinical course. Neuroradiology 53:939–945. doi:10.1007/s00234-010-0820-4
36. Tomiyasu M, Aida N, Watanabe Y et al (2012) Monitoring the brain metabolites of children with acute encephalopathy caused by the H1N1 virus responsible for the 2009 influenza pandemic: a quantitative in vivo 1H MR spectroscopy study. Magn Reson Imaging 30:1527–1533. doi:10.1016/j.mri.2012.05.007
37. Mizuguchi M, Abe J, Mikkaichi K et al (1995) Acute necrotising encephalopathy of childhood: a new syndrome presenting with multifocal, symmetric brain lesions. J Neurol Neurosurg Psychiatry 58:555–561
38. Wong AM, Simon EM, Zimmerman RA et al (2006) Acute necrotizing encephalopathy of childhood: correlation of MR findings and clinical outcome. Am J Neuroradiol 27:1919–1923
39. Dale RC (2005) Post-streptococcal autoimmune disorders of the central nervous system. Dev Med Child Neurol 47:785–791. doi:10.1111/j.1469-8749.2005.tb01079.x
40. Rubio-Agustí I, Dalmau J, Sevilla T et al (2011) Isolated hemidystonia associated with NMDA receptor antibodies. Mov Disord 26:351–352. doi:10.1002/mds.23315
41. Kim S-H, Huh S-Y, Hyun J-W et al (2014) A longitudinal brain magnetic resonance imaging study of neuromyelitis optica spectrum disorder. PLoS ONE 9, e108320. doi:10.1371/journal.pone.0108320
42. Zuccoli G, Panigrahy A, Sreedher G et al (2014) Vasogenic edema characterizes pediatric acute disseminated encephalomyelitis. Neuroradiology 56:679–684. doi:10.1007/s00234-014-1379-2
43. Robertson WC, Smith CD (2002) Sydenham's chorea in the age of MRI: a case report and review. Pediatr Neurol 27:65–67
44. Swedo SE, Seidlitz J, Kovacevic M et al (2015) Clinical presentation of pediatric autoimmune neuropsychiatric disorders associated with streptococcal infections in research and community settings. J Child Adolesc Psychopharmacol 25:26–30. doi:10.1089/cap.2014.0073
45. Giedd JN, Rapoport JL, Garvey MA et al (2000) MRI assessment of children with obsessive-compulsive disorder or tics associated with streptococcal infection. Am J Psychiatry 157:281–283
46. Elia J, Dell ML, Friedman DF et al (2005) PANDAS with catatonia: a case report. Therapeutic response to lorazepam and plasmapheresis. J Am Acad Child Adolesc Psychiatry 44:1145–1150. doi:10.1097/01.chi.0000179056.54419.5e
47. Kumar A, Williams MT, Chugani HT (2015) Evaluation of basal ganglia and thalamic inflammation in children with pediatric autoimmune neuropsychiatric disorders associated with streptococcal infection and Tourette syndrome: a positron emission tomographic (PET) study using 11C-[R]-PK11195. J Child Neurol 30:749–756. doi:10.1177/0883073814543303
48. Ben Azoun M, Tatencloux S, Deiva K, Blanc P (2014) Two pediatric cases of anti-NMDA receptor antibody encephalitis. Arch Pédiatr 21:1216–1219. doi:10.1016/j.arcped.2014.08.020
49. Tzoulis C, Vedeler C, Haugen M et al (2013) Progressive striatal necrosis associated with anti-NMDA receptor antibodies. BMC Neurol 13:55. doi:10.1186/1471-2377-13-55
50. Lennon VA, Kryzer TJ, Pittock SJ et al (2005) IgG marker of optic-spinal multiple sclerosis binds to the aquaporin-4 water channel. J Exp Med 202:473–477. doi:10.1084/jem.20050304
51. Wingerchuk DM, Lennon VA, Pittock SJ et al (2006) Revised diagnostic criteria for neuromyelitis optica. Neurology 66:1485–1489
52. Tenembaum S, Chitnis T, Ness J, Hahn JS, International Pediatric MS Study Group (2007) Acute disseminated encephalomyelitis. Neurology 68:S23–S36. doi:10.1212/01.wnl.0000259404.51352.7f
53. Krupp LB, Banwell B, Tenembaum S et al (2007) Consensus definitions proposed for pediatric multiple sclerosis and related disorders. Neurology 68:S7–S12
54. Schor NF (2000) Neurology of systemic autoimmune disorders: a pediatric perspective. Semin Pediatr Neurol 7:108–117
55. Zuccoli G, Crowley H, Cecil KM (2013) Inherited metabolic and neurodegenerative disorders. In: Caffeys Pediatr. Diagn. Imaging, 12th edn. Elsevier Health Sciences, Philadelphia, pp 330–357
56. Autti T, Joensuu R, Aberg L (2007) Decreased T2 signal in the thalami may be a sign of lysosomal storage disease. Neuroradiology 49:571–578. doi:10.1007/s00234-007-0220-6
57. Provenzale JM, Barboriak DP, Sims K (1995) Neuroradiologic findings in fucosidosis, a rare lysosomal storage disease. Am J Neuroradiol 16:809–813
58. Arii J, Tanabe Y (2000) Leigh syndrome: serial MR imaging and clinical follow-up. AJNR Am J Neuroradiol 21:1502–1509
59. Warmuth-Metz M, Hofmann E, Büsse M, Solymosi L (1999) Uncommon morphologic characteristics in Leigh's disease. AJNR Am J Neuroradiol 20:1158–1160
60. Sener RN (2004) Diffusion magnetic resonance imaging patterns in metabolic and toxic brain disorders. Acta Radiol 45:561–570
61. Rossi A, Biancheri R, Bruno C et al (2003) Leigh syndrome with COX deficiency and SURF1 gene mutations: MR imaging findings. Am J Neuroradiol 24:1188–1191
62. Krägeloh-Mann I, Grodd W, Schöning M et al (1993) Proton spectroscopy in five patients with Leigh's disease and mitochondrial enzyme deficiency. Dev Med Child Neurol 35:769–776
63. Brismar J, Ozand PT (1995) CT and MR of the brain in glutaric acidemia type I: a review of 59 published cases and a report of 5 new patients. AJNR Am J Neuroradiol 16:675–683
64. Desai NK, Runge VM, Crisp DE et al (2003) Magnetic resonance imaging of the brain in glutaric acidemia type I: a review of the literature and a report of four new cases with attention to the basal ganglia and imaging technique. Investig Radiol 38:489–496. doi:10.1097/01.rli.0000080405.62988.f6
65. Manoli I, Venditti CP (1993) Methylmalonic acidemia. GeneReviews(®)
66. Baumgarter ER, Viardot C (1995) Long-term follow-up of 77 patients with isolated methylmalonic acidaemia. J Inherit Metab Dis 18:138–142
67. Sobrido MJ, Coppola G, Oliveira J, et al. (1993) Primary familial brain calcification. GeneReviews(®)
68. Livingston JH, Stivaros S, van der Knaap MS, Crow YJ (2013) Recognizable phenotypes associated with intracranial calcification. Dev Med Child Neurol 55:46–57. doi:10.1111/j.1469-8749.2012.04437.x
69. Illum F, Dupont E (1985) Prevalences of CT-detected calcification in the basal ganglia in idiopathic hypoparathyroidism and pseudohypoparathyroidism. Neuroradiology 27:32–37
70. Brunetti-Pierri N, Scaglia F (2008) GM1 gangliosidosis: review of clinical, molecular, and therapeutic aspects. Mol Genet Metab 94:391–396. doi:10.1016/j.ymgme.2008.04.012

71. Regier DS, Tifft CJ (1993) GLB1-related disorders. GeneReviews(®)
72. Erol I, Alehan F, Pourbagher MA et al (2006) Neuroimaging findings in infantile GM1 gangliosidosis. Eur J Paediatr Neurol 10: 245–248. doi:10.1016/j.ejpn.2006.08.005
73. Kaback MM, Desnick RJ (1993) Hexosaminidase A deficiency. GeneReviews(®)
74. Kroll RA, Pagel MA, Roman-Goldstein S et al (1995) White matter changes associated with feline GM2 gangliosidosis (Sandhoff disease): correlation of MR findings with pathologic and ultrastructural abnormalities. AJNR Am J Neuroradiol 16:1219–1226
75. Yüksel A, Yalçinkaya C, Işlak C et al (1999) Neuroimaging findings of four patients with Sandhoff disease. Pediatr Neurol 21: 562–565
76. Chen CY, Zimmerman RA, Lee CC et al (1998) Neuroimaging findings in late infantile GM1 gangliosidosis. AJNR Am J Neuroradiol 19:1628–1630
77. Wilken B, Dechent P, Hanefeld F, Frahm J (2008) Proton MRS of a child with Sandhoff disease reveals elevated brain hexosamine. Eur J Paediatr Neurol 12:56–60. doi:10.1016/j.ejpn.2007.05.008
78. Jan W, Zimmerman RA, Wang ZJ et al (2003) MR diffusion imaging and MR spectroscopy of maple syrup urine disease during acute metabolic decompensation. Neuroradiology 45:393–399. doi:10.1007/s00234-003-0955-7
79. Ha JS, Kim T-K, Eun B-L et al (2004) Maple syrup urine disease encephalopathy: a follow-up study in the acute stage using diffusion-weighted MRI. Pediatr Radiol 34:163–166. doi:10.1007/s00247-003-1058-7
80. Brismar J, Aqeel A, Brismar G et al (1990) Maple syrup urine disease: findings on CT and MR scans of the brain in 10 infants. Am J Neuroradiol 11:1219–1228
81. Sato T, Muroya K, Hanakawa J et al (2014) Neonatal case of classic maple syrup urine disease: usefulness of (1) H-MRS in early diagnosis. Pediatr Int 56:112–115. doi:10.1111/ped.12211
82. Heindel W, Kugel H, Wendel U et al (1995) Proton magnetic resonance spectroscopy reflects metabolic decompensation in maple syrup urine disease. Pediatr Radiol 25:296–299
83. Yalcinkaya C, Benbir G, Salomons GS et al (2005) Atypical MRI findings in Canavan disease: a patient with a mild course. Neuropediatrics 36:336–339. doi:10.1055/s-2005-872878
84. Janson CG, McPhee SWJ, Francis J et al (2006) Natural history of Canavan disease revealed by proton magnetic resonance spectroscopy (1H-MRS) and diffusion-weighted MRI. Neuropediatrics 37:209–221. doi:10.1055/s-2006-924734
85. Tissières P, Chevret L, Debray D, Devictor D (2003) Fulminant Wilson's disease in children: appraisal of a critical diagnosis. Pediatr Crit Care Med 4:338–343. doi:10.1097/01.PCC.0000074268.77622.DE
86. Yüce A, Koçak N, Demir H et al (2003) Evaluation of diagnostic parameters of Wilson's disease in childhood. Indian J Gastroenterol 22:4–6
87. Dhawan A, Taylor RM, Cheeseman P et al (2005) Wilson's disease in children: 37-year experience and revised King's score for liver transplantation. Liver Transpl 11:441–448. doi:10.1002/lt.20352
88. Arnon R, Calderon JF, Schilsky M et al (2007) Wilson disease in children: serum aminotransferases and urinary copper on triethylene tetramine dihydrochloride (trientine) treatment. J Pediatr Gastroenterol Nutr 44:596–602. doi:10.1097/MPG.0b013e3180467715
89. Marcellini M, Di Ciommo V, Callea F et al (2005) Treatment of Wilson's disease with zinc from the time of diagnosis in pediatric patients: a single-hospital, 10-year follow-up study. J Lab Clin Med 145:139–143
90. Kumagi T, Horiike N, Michitaka K et al (2004) Recent clinical features of Wilson's disease with hepatic presentation. J Gastroenterol 39:1165–1169. doi:10.1007/s00535-004-1466-y
91. Ferenci P, Caca K, Loudianos G et al (2003) Diagnosis and phenotypic classification of Wilson disease. Liver Int 23:139–142
92. Sánchez-Albisua I, Garde T, Hierro L et al (1999) A high index of suspicion: the key to an early diagnosis of Wilson's disease in childhood. J Pediatr Gastroenterol Nutr 28:186–190
93. Tarnacka B, Szeszkowski W, Gołębiowski M, Członkowska A (2010) Brain proton magnetic spectroscopy in long-term treatment of Wilson's disease patients. Metab Brain Dis 25:325–329. doi:10.1007/s11011-010-9214-x
94. Nicolas G, Devys D, Goldenberg A et al (2011) Juvenile Huntington disease in an 18-month-old boy revealed by global developmental delay and reduced cerebellar volume. Am J Med Genet A 155:815–818. doi:10.1002/ajmg.a.33911
95. Reynolds NC, Prost RW, Mark LP, Joseph SA (2008) MR-spectroscopic findings in juvenile-onset Huntington's disease. Mov Disord 23:1931–1935. doi:10.1002/mds.22245
96. Straussberg R, Shorer Z, Weitz R et al (2002) Familial infantile bilateral striatal necrosis Clinical features and response to biotin treatment. Neurology 59:983–989
97. Kornreich L, Bron-Harlev E, Hoffmann C et al (2005) Thiamine deficiency in infants: MR findings in the brain. AJNR Am J Neuroradiol 26:1668–1674
98. Zeng W-Q, Al-Yamani E, Acierno JS et al (2005) Biotin-responsive basal ganglia disease maps to 2q36.3 and is due to mutations in SLC19A3. Am J Hum Genet 77:16–26. doi:10.1086/431216
99. Haacke EM, Ayaz M, Khan A et al (2007) Establishing a baseline phase behavior in magnetic resonance imaging to determine normal vs. abnormal iron content in the brain. J Magn Reson Imaging 26:256–264. doi:10.1002/jmri.22987
100. Gregory A, Hayflick SJ (2011) Genetics of neurodegeneration with brain iron accumulation. Curr Neurol Neurosci Rep 11: 254–261. doi:10.1007/s11910-011-0181-3
101. Hayflick SJ, Hartman M, Coryell J et al (2006) Brain MRI in neurodegeneration with brain iron accumulation with and without PANK2 mutations. AJNR Am J Neuroradiol 27:1230–1233
102. Morgan NV, Westaway SK, Morton JEV et al (2006) PLA2G6, encoding a phospholipase A2, is mutated in neurodegenerative disorders with high brain iron. Nat Genet 38:752–754. doi:10.1038/ng1826
103. Kurian MA, Morgan NV, MacPherson L et al (2008) Phenotypic spectrum of neurodegeneration associated with mutations in the PLA2G6 gene (PLAN). Neurology 70:1623–1629. doi:10.1212/01.wnl.0000310986.48286.8e
104. Illingworth MA, Meyer E, Chong WK et al (2014) PLA2G6-associated neurodegeneration (PLAN): further expansion of the clinical, radiological and mutation spectrum associated with infantile and atypical childhood-onset disease. Mol Genet Metab 112: 183–189. doi:10.1016/j.ymgme.2014.03.008
105. Pagon RA, Adam MP, Ardinger HH, et al., others (2014) Neurodegeneration with brain iron accumulation disorders overview
106. Sechi G, Serra A (2007) Wernicke's encephalopathy: new clinical settings and recent advances in diagnosis and management. Lancet Neurol 6:442–455. doi:10.1016/S1474-4422(07)70104-7
107. Harper CG, Giles M, Finlay-Jones R (1986) Clinical signs in the Wernicke-Korsakoff complex: a retrospective analysis of 131 cases diagnosed at necropsy. J Neurol Neurosurg Psychiatry 49: 341–345
108. Vasconcelos MM, Silva KP, Vidal G et al (1999) Early diagnosis of pediatric Wernicke's encephalopathy. Pediatr Neurol 20:289–294

109. Gallucci M, Bozzao A, Splendiani A et al (1990) Wernicke encephalopathy: MR findings in five patients. AJNR Am J Neuroradiol 11:887–892
110. Zuccoli G, Santa Cruz D, Bertolini M et al (2009) MR imaging findings in 56 patients with Wernicke encephalopathy: nonalcoholics may differ from alcoholics. AJNR Am J Neuroradiol 30: 171–176. doi:10.3174/ajnr.A1280
111. Zuccoli G, Siddiqui N, Bailey A, Bartoletti SC (2010) Neuroimaging findings in pediatric Wernicke encephalopathy: a review. Neuroradiology 52:523–529. doi:10.1007/s00234-009-0604-x
112. Ozand PT, Gascon GG, Al Essa M et al (1998) Biotin-responsive basal ganglia disease: a novel entity. Brain J Neurol 121(Pt 7): 1267–1279
113. Tabarki B, Al-Shafi S, Al-Shahwan S et al (2013) Biotin-responsive basal ganglia disease revisited: clinical, radiologic, and genetic findings. Neurology 80:261–267. doi:10.1212/WNL.0b013e31827deb4c
114. Zuccoli G, Pipitone N (2009) Neuroimaging findings in acute Wernicke's encephalopathy: review of the literature. AJR Am J Roentgenol 192:501–508. doi:10.2214/AJR.07.3959
115. Batshaw ML, Tuchman M, Summar M, Seminara J, Members of the Urea Cycle Disorders Consortium (2014) A longitudinal study of urea cycle disorders. Mol Genet Metab 113:127–130. doi:10.1016/j.ymgme.2014.08.001
116. Bireley WR, Van Hove JLK, Gallagher RC, Fenton LZ (2012) Urea cycle disorders: brain MRI and neurological outcome. Pediatr Radiol 42:455–462. doi:10.1007/s00247-011-2253-6
117. Gropman A (2010) Brain imaging in urea cycle disorders. Mol Genet Metab 100(Suppl 1):S20–S30. doi:10.1016/j.ymgme.2010.01.017
118. Gunz AC, Choong K, Potter M, Miller E (2013) Magnetic resonance imaging findings and neurodevelopmental outcomes in neonates with urea-cycle defects. Int Med Case Rep J 6:41–48. doi:10.2147/IMCRJ.S43513
119. Pacheco-Colón I, Fricke S, VanMeter J, Gropman AL (2014) Advances in urea cycle neuroimaging: Proceedings from the 4th International Symposium on urea cycle disorders, Barcelona, Spain, September 2013. Mol Genet Metab 113:118–126. doi:10.1016/j.ymgme.2014.05.005
120. Ranger AM, Chaudhary N, Avery M, Fraser D (2012) Central pontine and extrapontine myelinolysis in children: a review of 76 patients. J Child Neurol 27:1027–1037. doi:10.1177/0883073812445908
121. Ruzek KA, Campeau NG, Miller GM (2004) Early diagnosis of central pontine myelinolysis with diffusion-weighted imaging. Am J Neuroradiol 25:210–213
122. Swoboda KJ, Saul JP, McKenna CE et al (2003) Aromatic L-amino acid decarboxylase deficiency: overview of clinical features and outcomes. Ann Neurol 54(Suppl 6):S49–S55. doi:10.1002/ana.10631
123. Gibson KM, Christensen E, Jakobs C et al (1997) The clinical phenotype of succinic semialdehyde dehydrogenase deficiency (4-hydroxybutyric aciduria): case reports of 23 new patients. Pediatrics 99:567–574
124. Parviz M, Vogel K, Gibson KM, Pearl PL (2014) Disorders of GABA metabolism: SSADH and GABA-transaminase deficiencies. J Pediatr Epilepsy 3:217–227. doi:10.3233/PEP-14097
125. Yalçinkaya C, Gibson KM, Gündüz E et al (2000) MRI findings in succinic semialdehyde dehydrogenase deficiency. Neuropediatrics 31:45–46